Electronic Supplementary Material (ESI) for Journal of Materials Chemistry A.

porting Information

Nano-confined Multi-synthesis of Li-Mg-N-H Nanocomposite towards Low-temperature Hydrogen Storage with Stable Reversiblity

Guanglin Xia,[a,b] Xiaowei Chen,[b] Cuifeng Zhou,[d] Chaofeng Zhang,[a] Dan Li,[a] Qinfen Gu,[c] Zaiping Guo*[a] Huakun Liu[a] Zongwen Liu[d] and Xuebin Yu*[b]

[a] *Institute for Superconducting and Electronic Materials, University of Wollongong, Wollongong, Australia.*

[b] *Department of Materials Science, Fudan University, Shanghai, China.*

[c] *Australian Synchrotron, 800 Blackburn Rd., Clayton 3168, Australia.*

[d] *School of Chemical and Biomolecular Engineering, The University of Sydney, Sydney, Australia.*

Experimental details

Synthesis of SnO_2 hollow spheres: The hollow SnO_2 nanoparticles were prepared using a simple hydrothermal method in an ethanol-H_2O mixed solvent [1]. In a typical synthesis, urea (0.36 g, 0.1 M) additive was firstly dissolved in 60 mL of ethanol/water mixed solvent with a volume ratio of 3:5. Thereafter, 0.288 g potassium stannate trihydrate ($K_2SnO_3 \cdot 3H_2O$, Sigma-Aldrich, 99.9%) was slowly added, followed by gentle shaking by hand for around 3 min until a translucent solution was obtained, which was then transferred into a 100 mL Teflon-lined stainless steel autoclave and heated at 200 °C for 20 h in an electric oven. The autoclave was then taken out of the oven and left to cool down to room temperature. The white precipitate was collected by centrifugation, washed thoroughly with water several times, and then dried at 60 °C overnight.

Synthesis of thin-film hollow carbon spheres: The carbon spheres were obtained by coating glucose on the SnO_2 hollow spheres by a simple hydrothermal process. In a typical synthesis, 0.1 g of the as-prepared SnO_2 hollow spheres was easily dispersed by ultrasonication in 20 mL of 0.5 M aqueous glucose solution. The suspension was then transferred into a 40 mL Teflon-lined autoclave and kept in an electric oven at 180 ^{o}C for 4 h. The product was harvested by centrifugation and washed with deionized water and ethanol several times. After drying at 60 ^{o}C for around 5 h, the brown powder was heated to 650 ^{o}C for 5 h in flowing H_2/N_2 (v/v = 10:90) with a heating rate of 1 ^{o}C min^{-1}. Following that, the product was dispersed in 2 M HCl to remove the residual Sn particles, and the double-shelled hollow carbon spheres (THCSs) were collected by centrifugation, followed by drying at 60 ^{o}C overnight.

Preparation of the nanoconfined Li-Mg-N-H composite in THCSs: Selected THCSs were firstly activated at 500 ^{o}C under vacuum for several hours in order to remove moisture and gases from the porous matrix. Subsequently, a solution of LiN_3 and $MgCl_2$ with a molar ratio of 2:1 in 2,2,2-trifluoroethanol (TFE, CF_3CH_2OH), which was stirred in advance for around 5 h to ensure the homogeneous mixing of raw materials, was added to the pre-activated THCSs. After 0.5 h of infiltration via the capillary effect, the sample was vacuum dried at 150 ^{o}C for 10 h to remove the solvent. To produce a space-confined nanocomposite with a relatively high loading capacity and good dispersion of the starting materials inside the nanopores of the THCSs, several successive steps of infiltration/vacuum-drying were conducted followed by washing with pure TFE and drying. Afterwards, the nanoconfined precursors were dried at 150 ^{o}C and then activated under 150 bar hydrogen pressure at 200 ^{o}C for 12 h by a metathesis reaction, as illustrated in Figure 1, which results in the formation of Li-Mg-N-H composite. According to elemental analysis, the resulting composite contained 15.79 mass% Li, 9.23 mass% Mg, 10.59 mass% N and 35.41 mass% C, which gives the mass concentration of $Li_2Mg(NH)_2$ to be ~ 25.8 mass% in the as-prepared products based on the combination of molar ratio in the raw precursors and the reaction mechanism.

Materials characterization: Mass spectrometry (MS; Hidden HPR 20) was conducted from room temperature, using a heating rate of 2 ^{o}C min^{-1} under dynamic nitrogen with a purge rate of 80 ml min^{-1}. Differential scanning calorimetry (DSC) measurements were performed using a TAQ 2000 DSC under N_2 with a gas flow of 40 mL min^{-1} at a heating rate of 2 ^{o}C min^{-1}. Nitrogen absorption/desorption isotherms (Brunauer-Emmett-Teller (BET) technique) at the temperature of liquid nitrogen via a Quantachrome NOVA 4200e instrument were collected to characterize the pore structure of the samples. According to the Barrett-Jouner-Halenda (BJH) model from the adsorption branches of isotherms, the pore volumes and pore size distributuions were determined. The phase composition of the powders was analyzed by X-ray diffraction (XRD, D8 Advance, Bruker AXS) with Cu Kα radiation. Amorphous tape was used to prevent any possible reactions between the sample and air during the XRD measurement. High-resolution X-ray diffraction data were collected using a Mythen-II detector with a wavelength of 0.8266 Å at the Powder Diffraction Beamline, Australian Synchrotron. The sample was loaded into a pre-dried 0.7 mm boron-silica glass capillary tube, and the capillary tube was then sealed with vacuum grease in a glove box filled with argon. The time-resolved in-situ measurements were conducted using a Cyberstar hot-air blower to heat the capillary to the targeted temperature at a constant heating rate of 2 ^{o}C min^{-1}. Fourier transform infrared (FTIR, Magna-IR 550 II, Nicolet) analysis was conducted to determine the chemical bonding. During the FTIR measurements (KBr pellets), samples were loaded into a closed tube with KBr for measurement in an argon-filled glove box. The morphology of the samples was evaluated using a field emission scanning electron microscope (FE-SEM, JEOL 7500FA, Tokyo, Japan) and a transmission electron microscope (TEM, JEOL 2011 F, Tokyo, Japan). Elemental analysis was performed with an Elemen Tar Vario EL3 Elemental Analyser.

The hydrogen storage properties of the nanoconfined Li-Mg-N-H composite were examined with the aid of a Sieverts' apparatus, identified as a gas reaction controller (GRC, Advanced Materials Corp., USA). The apparatus was carefully calibrated from the H_2 sorption of a

$LaNi_5$ reference sample with an accuracy of ±1%, and, typically, a ~500 mg sample was loaded into a stainless-steel autoclave for hydrogenation and dehydrogenation measurements. The H_2 absorption kinetics measurements were performed at various temperatures with an initial pressure of 35 atm, and the desorption properties were detected at various temperatures under hydrogen pressure below 0.02 atm. The pressure-concentration isotherm (PCI) measurements were performed at the desired temperatures, and the equilibrium time for each point was 600 s. For comparison, the amount of hydrogen released from the nanoconfined composite is based on the composite of $Mg(NH_2)_2$-2LiH, while the THCSs, LiCl, and extra LiH are excluded.

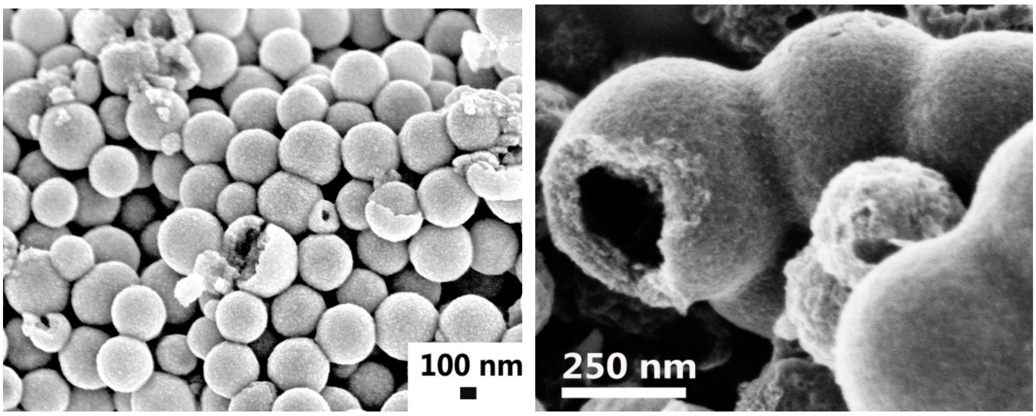

Figure S1. FESEM images of the as-prepared SnO_2 hollow spheres (left) and THCSs (right). Some of the hollow spheres are cracked, exhibiting the exposed interior.

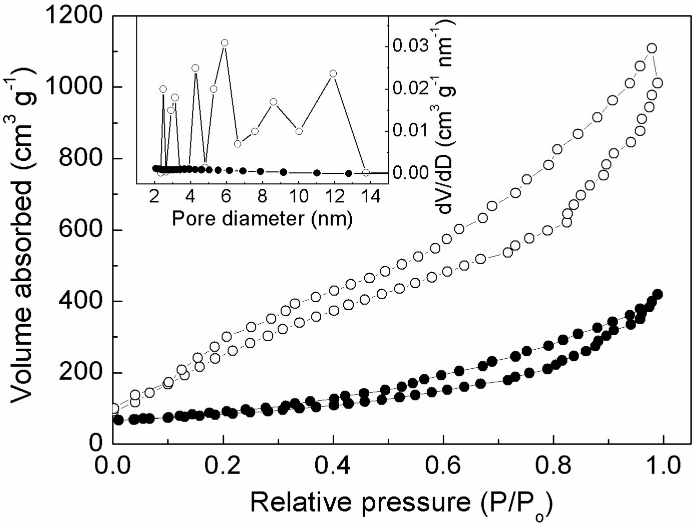

Figure S2. Nitrogen isotherms and pore size distribution (inset) of the freshly-prepared THCSs (○) and the THCSs with the loading of Li-Mg-N-H composite (●).

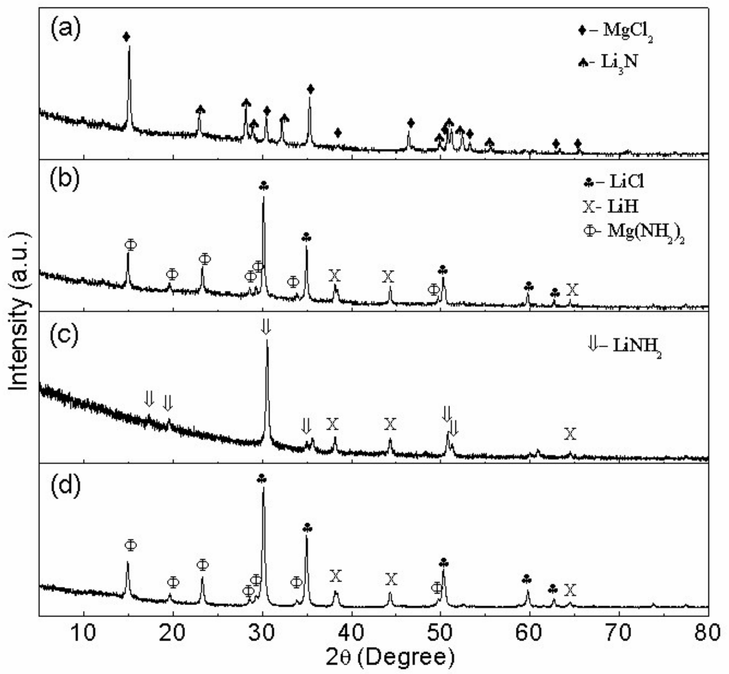

Figure S3. XRD patterns of (a) the vacuum-dried products from the precursors of $MgCl_2$ and LiN_3 heat-treated at 200 ^{o}C and (b) the products after annealing at 200 ^{o}C under 150 bar of H_2, (c) Li_3N after annealing at 200 ^{o}C under 150 bar of H_2, and (d) the mixed composite of $MgCl_2$ with the hydrogenated Li_3N after annealing at 200 ^{o}C under 150 bar of H_2.

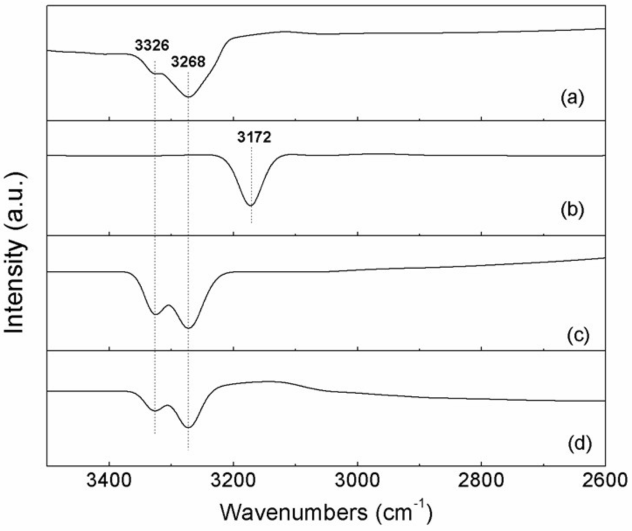

Figure S4. FTIR spectra of the nanoconfined Li-Mg-N-H nanoparticles (a), and the products after the 1st dehydrogenation (b), 1st hydrogenation (c), and 20th hydrogenation (d).

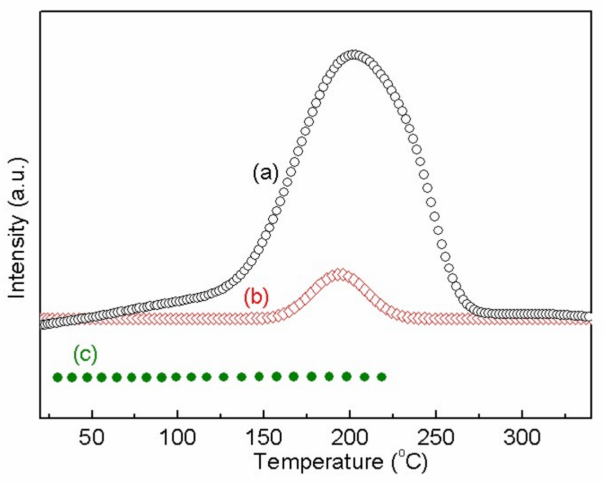

Figure S5. NH_3 signals of mass spectra during the decomposition of (a) nanoconfined Li-Mg-N-H composite compared with ball-milled composite of (b) $Mg(NH_2)_2$-2LiH and (c) $Mg(NH_2)_2$-4LiH, respectively.

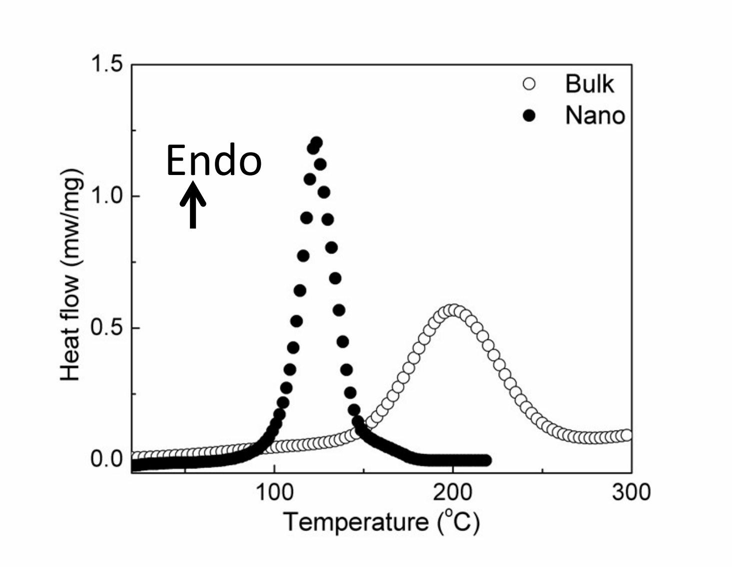

Figure S6. DSC curve of the nanoconfined Li-Mg-N-H nanoparticles (Nano) compared with their ball-milled counterpart (Bulk), obtained with a heating rate of 2 ^{o}C min^{-1} under dynamic N_2.

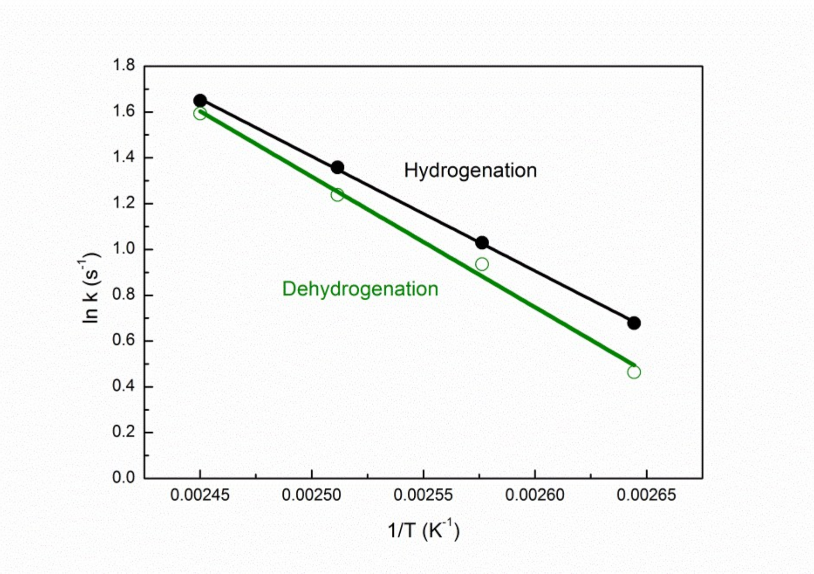

Figure S7. Arrhenius plots for the isothermal hydrogenation and dehydrogenation of the nanoconfined Li-Mg-N-H composite.

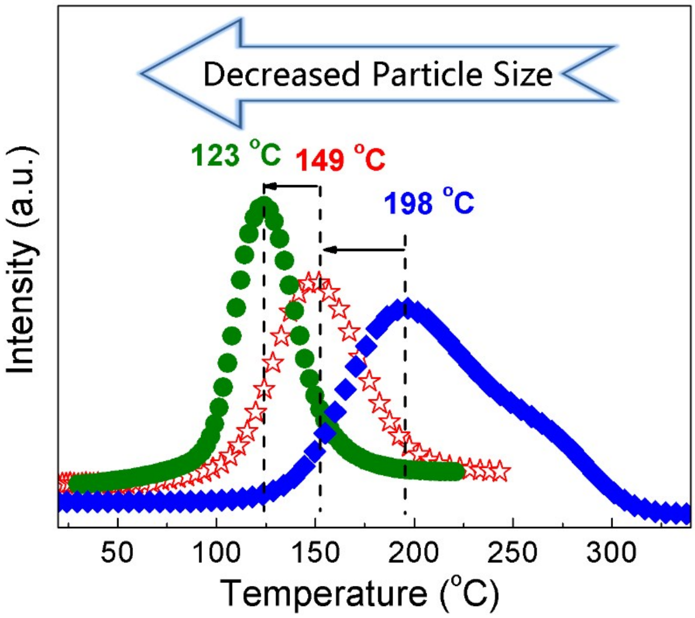

Figure S8. Mass spectra of the nanoconfined $Li_2Mg(NH)_2$ with a loading capacity of 25.8 wt.% (●) and 32.1 wt.% (☆), respectively, as compared with bulk $Li_2Mg(NH)_2$ (♦)

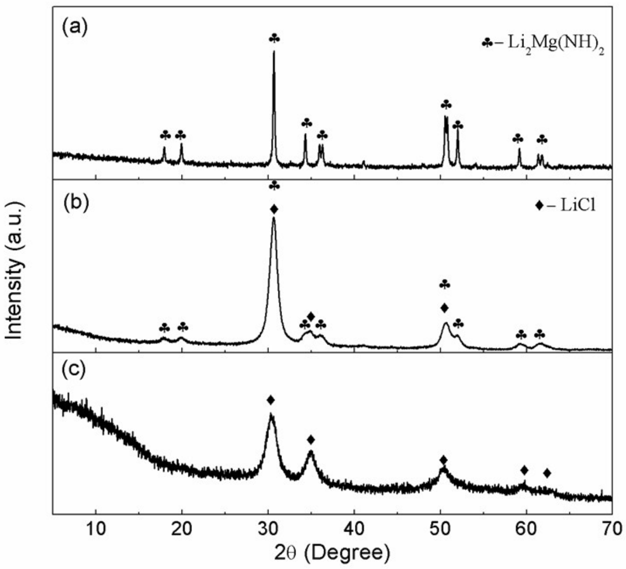

Figure S9. Regular XRD spectra of the dehydrogenated products: (a) the ball-milled Li-Mg-N-H composite, and the nanoconfined Li-Mg-N-H composite with a loading capacity of 32.1% (b) and 25.8% (c), respectively.

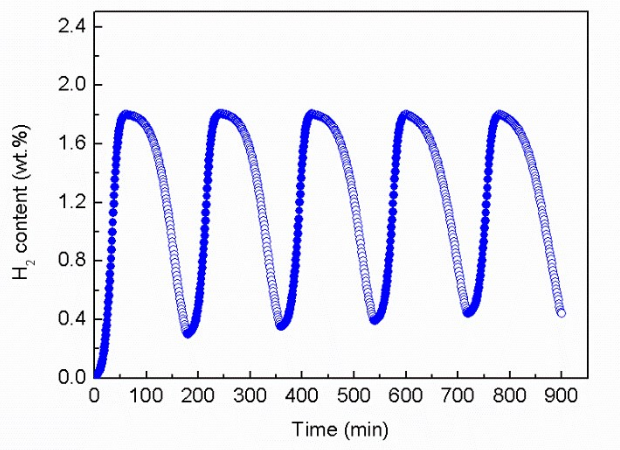

Figure S10. Reversible H_2 absorption and desorption of nanoconfined Li-Mg-N-H composite with a loading capacity of 50% at 135 ^{o}C.

References:

[1] C. F. Zhang, H. B. Wu, C. Z. Yuan, Z. P. Guo, and X. W. Lou, *Angew. Chem. Int. Ed.*, 2012, **51**, 9592.